THE ASTROPHYSICAL JOURNAL, 421:236–244, 1994 January 20

HOT OR NOT? THEORETICAL BLUE EDGES FOR DA AND DB WHITE DWARF MODELS

P. A. BRADLEY[1] AND D. E. WINGET
McDonald Observatory and Department of Astronomy, University of Texas at Austin, Austin, TX 78712-1083
Received 1993 June 1; accepted 1993 July 30

ABSTRACT

We present the nonadiabatic results of a parametric survey of compositionally stratified evolutionary white dwarf models of with helium surface layers (DB white dwarfs) and hydrogen surface layers (DA white dwarfs). We examine the effect of varying the stellar mass, varying the hydrogen and helium layer masses, and the treatment of convection on the temperature of the theoretical blue edge.

In general, the blue edge is relatively insensitive to the helium or hydrogen layer mass. The exception occurs for DB models with helium layer masses less than $10^{-8}M_*$; they are pulsationally stable at all temperatures. We find the blue edge is very sensitive to the treatment of convection, consistent with previous results. The most efficient treatment of convection we consider yields a blue edge near 27,000 K for our 0.6 $M_\odot$ DB model and near 12,700 K for our 0.6 $M_\odot$ DA models. Thus, we can match the observed DB blue edge located between 24,000–25,000 K by tuning the convective efficiency. The temperature of our theoretical DA blue edges for 0.6 $M_\odot$ models with efficient version of convection are similar to the observed blue edge. For both DA and DB models, there is a slight dependence of the blue edge on stellar mass, with higher mass models having hotter blue edges. The change in blue edge with stellar mass may offer an explanation for the existence of nonpulsators within the instability strip.

Subject headings: stars: evolution — stars: interiors — stars: oscillations — white dwarfs

1. INTRODUCTION

Asteroseismology of white dwarf (WD) stars gives us the potential to determine the structure of their cores and envelopes (see Winget 1993, 1991, 1988a, b; Kawaler 1990; Kawaler & Hansen 1989). Knowing the internal structure of white dwarf stars will then open the way to a better understanding of many pressing problems in astrophysics. Asteroseismology can help shed light on the structure of the partial ionization zone where pulsation driving occurs, a critical—and ill-understood—region inside a white dwarf. Seismology using the adiabatic pulsation period distribution works best in regions where the weight function (see Kawaler, Hansen, & Winget 1985; Epstein 1950) is a maximum, which is below the partial ionization zone of white dwarf stars. However, we can use the nonadiabatic pulsation properties of these stars to constrain the properties of the driving region. Here, we make a first pass at the problem by determining the location of the hot (blue) edge of the theoretical DA and DB instability strips and determine their sensitivity to various model parameters. Once we know the gross properties of the instability strips, we can set the stage for further progress with models utilizing improved treatments of convection and including convection-pulsation interactions in the nonradial pulsation equations.

We know of seven pulsating helium atmosphere (DBV) white dwarfs, all of which occupy an instability strip spanning $21{,}500 \lesssim T_{\rm eff} \lesssim 24{,}000$ K (Thejl, Vennes, & Shipman 1991). The 22 known DAV stars are pulsating hydrogen atmosphere white dwarfs, located between 13,000 and 11,000 K (Bergeron, Wesemael, & Fontaine 1992b; Wesemael et al. 1991; Daou et al. 1990; Lamontagne et al. 1989; Wesemael, Lamontagne, & Fontaine 1986). Theoretical studies show the pulsations are driven by the κ, γ mechanism in the surface helium (DBV stars) or hydrogen (DAV stars) partial-ionization zone, although convection-pulsation interactions play a poorly understood role (Brickhill 1983, 1991).

Observations suggest that a significant fraction of the DB and DA stars pulsate as they pass through the instability strip (Thejl et al. 1991; Liebert et al. 1986; Fontaine et al. 1985), and that the pulsators are otherwise normal DA and DB white dwarfs which are unstable to nonradial g-mode oscillations as they cool through the instability strip, where helium (DBV) or hydrogen (DAV) starts to recombine in their outer layers. However, there is growing evidence (see Kepler & Nelan 1993; Dolez, Vauclair, & Koester 1991) that not all of the DA white dwarfs in the instability strip pulsate. The imprecise temperature scale and small number of DB white dwarfs mean we cannot make the same statement about the pulsating DB white dwarfs. While we might expect a few nonpulsators within the instability strip because of an unfavorable observing geometry, we need to find other reasons for nonpulsators within the DA instability strip if they number more than a few percent.

There is considerable uncertainty concerning the final mass of the helium layer in the DBV white dwarfs and the hydrogen layer mass in the DAV white dwarfs. Evolutionary calculations of planetary nebula nuclei suggest that helium shell burning limits the final helium layer mass ($M_{\rm He}$) to be less than $10^{-2}M_*$, while the hydrogen layer mass ($M_{\rm H}$) must be less than $10^{-4}M_*$ to avoid fusion (see Iben 1991; D'Antona & Mazzitelli 1991; Blöcker & Schönberner 1991, and references therein). The final mass of the surface layer—be it hydrogen or helium—is highly dependent on where within the interval between helium shell flashes the last mass-loss episode occurs, so that essentially any helium or hydrogen layer mass is possible, with suitable adjustments to the theories.

An observational constraint of sorts on the helium layer mass of DB white dwarfs comes from an interpretation of the observed trend of carbon abundances in $T_{\rm eff} \sim 9000$ K DQ white dwarfs (dubbed the "carbon pollution" problem) by Pel-

[1] Postal address: X-2 Division, MS B220, Los Alamos National Laboratory, Los Alamos, NM 87545.

letier et al. (1986). Their results suggest the mean helium layer mass is $\sim 10^{-3.5(\pm 0.5)} M_*$—almost two orders of magnitude lower than the theoretical upper limit. Pelletier et al. also show that if the helium layer mass is less than $10^{-6} M_*$, mixing can occur, and the resulting object would have a carbon-rich atmosphere. Winget et al. (1983) carried out preliminary explorations of the nonadiabatic oscillation properties of evolutionary DB models, and showed that models with $M_{\rm He} = 10^{-4} M_*$ and $10^{-6} M_*$ have blue edges consistent with observations, assuming an appropriate choice for the convective efficiency. However, their model grid was not comprehensive enough to allow a full exploration of the theoretical blue edge dependence on model parameters.

There is much more controversy about the mass of the hydrogen layer in the DA stars and in particular, the ZZ Ceti stars. In addition to the previously mentioned maximum mass, there is a minimum hydrogen layer mass of $10^{-14} M_*$ required to avoid mixing with the underlying helium layer before reaching the DA instability strip. The spectral evolution theory of white dwarfs (Fontaine & Wesemael 1987, 1991), requires hydrogen layers thinner than $10^{-10} M_*$ to explain the observed change in the number of DA to non-DA white dwarfs. However, recent interpretations of available X-ray data (Vennes & Fontaine 1992) no longer demands that all of the hot DA white dwarfs have thin hydrogen layers. The results of Bergeron et al. (1990) suggest that the hydrogen layer is thin enough for some helium to mix into the hydrogen layer in DA white dwarfs below $\sim$11,000 K. However, the observed number ratios of helium to hydrogen are not matched by convective mixing models mentioned in Fontaine & Wesemael (1991). Also, Greenstein (1986) presents spectra of cool white dwarfs; hydrogen lines persist even down to 5000 K, although the atmospheres are helium-dominated. These observations suggest that until we can accurately describe how hydrogen and helium mix, the thickness of the hydrogen layer is still an open question.

Early nonadiabatic studies of DA models (see Winget 1981; Winget et al. 1982; Winget & Fontaine 1982; Bradley, Winget, & Wood 1989) suggested the theoretical blue edge is sensitive to the hydrogen layer mass. They found that only models with hydrogen layer masses between $10^{-12} M_*$ and $10^{-8} M_*$ have a blue edge near the observed one of 13,000 K, and the blue edge drops to about 8000 K when $M_{\rm H} > 10^{-8} M_*$. Our reanalysis of the same models used in the previous works shows that some of these model sequences have blue edges that are sensitive to the resolution of the driving region. This casts doubt on the reality of the trend, and stresses the need to examine the behavior of growth rates near the blue edge to see is there really is a change in the amount of damping present as the hydrogen layer mass changes.

Cox et al. (1987) disputes the need for thin hydrogen layers by showing that models with $M_{\rm H} = 10^{-4} M_*$—consistent with stellar evolution theory (Iben 1991; Koester & Schönberner 1986; D'Antona & Mazzitelli 1990)—have the same blue edge as models with thinner hydrogen layers, although they cannot get a blue edge hotter than 11,500 K without very large mixing length to pressure scale height ratios (Cox & Hollowell 1991). However, the stellar evolution value for the hydrogen layer mass is very sensitive to the particular phenomenological treatment of mass loss used. In addition, D'Antona & Mazzitelli (1991) demonstrate the need for the evolving models to include mass zones all the way from the center to the photosphere, to accurately account for gravitational contraction effects in outer layers where mass-loss occurs. These results underscore the theoretical sensitivity of the hydrogen layer mass to the behavior of the shell-burning sources during the final phases of mass loss and the lack of solid observational evidence to constrain competing theories. Further discussions about the expected structure of DB and DA white dwarfs are located in articles from recent meetings, such as Vauclair & Sion (1991), Wegner (1989), and Philip, Hayes, & Liebert (1987), and references therein.

We recently completed a comprehensive survey of the *adiabatic* properties of evolutionary DB white dwarf models constructed with an improved white dwarf evolutionary code (Bradley, Winget, & Wood 1993, hereafter BWW). We also examined a small set of DA models with the same code to determine the maximum rate of period change possible with carbon and oxygen core models (Bradley, Winget, & Wood 1992). Here, we extend our previous surveys to include the nonadiabatic properties of a grid of DA and DB models.

In the rest of the paper, we present our nonadiabatic results and compare the theoretical blue edges to observations. First, in § 2, we discuss our evolutionary white dwarf models and describe the numerical methods and accuracy checks we perform. In § 3, we present our nonadiabiatic results for evolutionary DA and DB white dwarf models. We close with a summary and conclusions, presented in § 4.

2. EQUILIBRIUM MODELS AND NUMERICAL METHODS

We use equilibrium models computed with the Rochester-Texas white dwarf evolution code (≡WDEC) described by Lamb & Van Horn (1975) and Wood (1990), with additional modifications to make them suitable for pulsation analysis. These models are the same as those used by Bradley et al. (1992, 1993), so we will only comment on a few details that are critical to the nonadiabatic pulsation properties of these models and refer the reader to the above references for further details.

We start our evolutionary sequences with the pure carbon core models of stars evolved from the main sequence to the planetary nebula nucleus stage used by Kawaler, Hansen, & Winget (1985). We evolve these models until the surface convection zone digs into the underlying helium (DA) or carbon (DB) layer or 2000–3000 K below the observed red edge, whichever comes first. We use 0.5 and 0.6 $M_\odot$ models for much of our analysis, bracketing the observational mean mass for DA and DB white dwarfs (Oke, Weidemann, & Koester 1984; Bergeron, Saffer, & Liebert 1992a). However, we also analyze models with masses ranging from 0.4 to 0.8 $M_\odot$ to investigate the effect of the stellar mass on the nonadiabatic pulsation properties.

We treat the mass of the hydrogen and helium layers as free parameters, using $10^{-2} M_* \leq M_{\rm He} \leq 10^{-10} M_*$ for the helium layer mass, while we allow the hydrogen layer mass to vary from $10^{-4} M_* \leq M_{\rm H} \leq 10^{-12} M_*$. In our DA models, we use a helium layer mass of $10^{-4} M_*$, to avoid model building problems at the core-envelope interface, except for a couple of cases where we use $10^{-2} M_*$. This approach is justified because we find that moving the He/C transition zone in a DA model has a small effect on the pulsation periods and the theoretical DA blue edge does not depend on the helium layer mass.

We model the hydrogen/helium (H/He) and helium/carbon (He/C) transition zones with a parameterization of the method of Arcouragi & Fontaine (1980), allowing the diffusion exponents to be free parameters. We use the abundance profile

predicted by diffusive equilibrium at the H/He transition zone, since our DA models are old enough for diffusive equilibrium to establish itself. We use the thick and thin He/C transition zones discussed by BWW in our DB models, because they are not old enough for diffusive equilibrium to be valid, except for the thinnest helium layers we examine. When $M_{\rm He} = 10^{-2}M_*$, we only use the thin He/C transition zones to avoid having helium present in the core of the model where it would burn explosively, in contradiction with the observations. We also use thin He/C transition zones in our DA models to avoid model building problems associated with having helium deep in the model and our DB model results show the He/C transition zone does not affect the nonadiabatic properties.

We use variations of mixing-length theory (ML) with different convective efficiencies described by Tassoul, Fontaine, & Winget (1990, hereafter TFW), of which ML3 is the most efficient. We use the Böhm & Cassinelli (1971) convection theory with $\alpha = 1$ (ML2) and $\alpha = 2$ (ML3) in most of our models, since TFW and Winget et al. (1982, 1983) show it matches the observed blue edges more closely. We also use different values of the mixing-length/pressure scale height ratio ($\equiv\alpha$) within the ML1 (Böhm-Vitense 1958) theory in an effort to match the models of CSKP more closely. In some of our models, we limit the convective efficiency via the prescription of Böhm & Stückl (1967), which sets the mixing-length as α pressure scale heights or the distance to the top of the convection zone, whichever is less. Model sequences using the Böhm and Stückl prescription are denoted by a "BS," while those that do not are labeled "NBS."

Because the κ, γ mechanism drives pulsations in DA and DB models, smooth opacities and opacity derivatives are essential for accurate nonadiabatic calculations. To this end, we modified the two-dimensional, fourth-order Lagrange interpolation opacity derivative subroutine written by H. Saio (see Winget et al. 1983) to handle multiple compositions and incorporated it into the white dwarf evolution code.

We use an extended form of the nomenclature system in BW and BWW as a shorthand way to describe the structure of our models. We specify the core composition, M_*, $M_{\rm He}$, $M_{\rm H}$, and convective efficiency via the following example: c/o60410ML2 refers to a C/O core 0.6 $M_\odot$ sequence with a helium layer mass of $10^{-4}M_*$ (the 04) and the hydrogen layer mass of $10^{-10}M_*$ (the 10). We prepend a "t" in front of the core composition of our DB sequences with thin He/C transition zones to distinguish them from their thick cousins.

We solve the nonradial oscillation equations in the form described by Saio & Cox (1980) using adiabatic and nonadiabatic pulsation analysis programs that employ a second-order Newton-Raphson relaxation technique, referred to as GNR1 (see Osaki & Hansen 1973, Winget 1981, Carroll 1981, and Unno et al. 1989 for details). We only consider $l = 1$ through 3 g-modes because we expect geometric cancellation effects to make $l > 3$ modes unobservable (Dziembowski 1977). We solve for the pulsation periods (P), kinetic energies of oscillation (K.E.), linear growth rates (γ), and eigenfunctions (y_1–y_6).

Because the low overtone g-modes become unstable first, we use them to locate the blue edge of the theoretical instability strip; these modes are also the least affected by changes in the resolution of the models. To determine the internal accuracy of our results, we use the variational principle applied to the computed eigenfunctions to determine an integrated period or growth rate. With this, the internal accuracy of the pulsation periods is about 1%–3%, while the growth rates agree to within a factor of 2 in most cases. The growth rate agreement is worse because only the outermost zones contribute to driving and damping of pulsations. Also, in these outer layers, the physical properties of the model change rapidly, making the integrated growth rate more susceptible to numerical noise. We also compute results for sample models with several different choices of zoning to ensure that our models have a sufficient number of zones for the eigenfunctions to be properly resolved. Here, the pulsation period differences are less than 0.1% for the low overtone modes we consider, while the growth rates agree to within a few percent until our models have so few zones (<200) that they are no longer adequately resolved.

A comparison of our pulsation periods to those of Bradley & Winget (1991) and Winget et al. (1983) reveals good agreement with our DB model periods, as discussed by BWW. Our DA model periods agree with those of Brassard et al. (1992) and Bradley & Winget (1991). The differences between our results and those of Cox et al. (1987) are already covered by Bradley et al. (1992) and Brassard et al. (1991). Our growth rates are similar to those we obtain from models used by Winget et al. (1982, 1983) and Winget (1981) and they follow similar trends. However, the agreement between the integrated and eigenvalue growth rates is worse in their results, due to poorer resolution in the driving region of their models.

3. NONADIABATIC RESULTS

Here, we discuss the nonadiabatic properties and theoretical blue edges of our evolutionary DB and DA white dwarf models and compare them to the observed instability strip. We are concerned with the location of the blue (hot) edge of the instability strip and how it changes as we vary the helium and hydrogen layer mass, convective efficiency, and stellar mass. We also examine how the mass of the helium layer (DB) and hydrogen layer (DA) affects the magnitude of the growth rate near the blue edge. Our nonadiabatic results allow us to make some global predictions about the structure of DBV and DAV white dwarfs, which we can test through asteroseismology of individual pulsators.

3.1. *DBV Model Results*

We begin by examining the location of the theoretical blue edge as we vary the helium layer mass for ML1, ML2, and ML3 convective efficiencies. When we use the Böhm-Stückl (BS) prescription limiting the convective efficiency, the blue edge moves from 20,000 K when we use inefficient (ML1) convection, through 23,000 K for ML2 convection, up to 24,600 K for very efficient (ML3) convection. When we do not use the Böhm-Stückl prescription, the ML2 blue edge is nearly 25,000 K, and the ML3 blue edge is about 27,000 K. There is no appreciable variation in the location of the blue edge due to changes in the helium layer mass, transition zone thickness, or core composition (see Table 1 and Fig. 1). Finally, Mazzitelli & D'Antona (1991) use a nonlocal description of convection (Canuto & Mazzitelli 1991) and obtain a blue edge near 25,000 K based on thermal timescale arguments, consistent with our sequences that incorporate moderately efficient convection.

Our ML3 (NBS) blue edge near 27,100 K lies in between the highest value of 28,600 K obtained by Winget et al. (1983) and the coldest value of 26,000 K found by Stanghellini, Cox, & Starrfield (1991). Cox et al. (1987) determine an intermediate value of 27,000 K. Cox et al. and Stanghellini et al. both used the Lagrangian pulsation analysis code of Pesnell (1990), which produces different pulsation periods than our pulsation analysis codes. They also use stellar structure models instead of

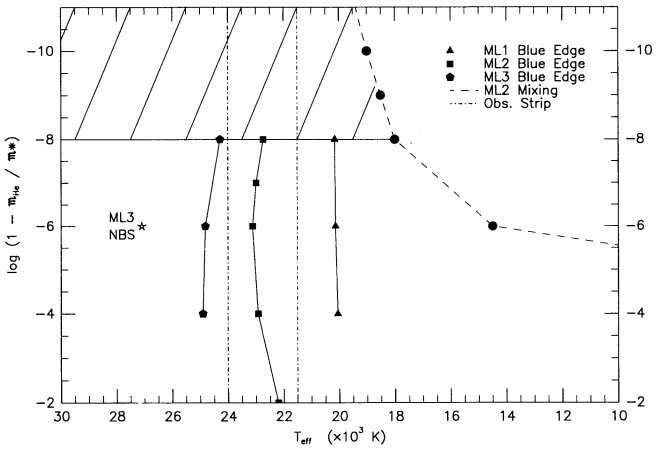

FIG. 1.—Location of the blue edge of the theoretical DB instability strip as a function of helium layer mass and convective efficiency. Models with ML2 NBS or ML3 BS (moderately efficient) convection best match the observed blue edge (*dash-dotted line*). The theoretical blue edge does not depend on the helium layer mass until $M_{\rm He} < 10^{-8}M_*$, (*hatched region*) when the extra damping below the driving region prevents pulsational instability from occurring. (See Fig. 2).

evolutionary models, which means their model for a 0.6 $M_\odot$ DB white dwarf at a given effective temperature may not have the same structure as an otherwise equivalent evolutionary model. The agreement between the blue edges of Cox et al. and Stanghellini et al. and ours implies their driving region structure is similar to ours.

We have two alternative explanations for the differences between our results and those of Winget et al. (1983), assuming it is significant. First, an order-of-magnitude calculation suggests that the size of the temperature gradient change due to our neglect of gravitational contraction may not be negligible, and it could be responsible for our blue edges being cooler than those of Winget et al. (1983) because the TFW models include these effects. In this sense, the TFW models analyzed by Winget et al. are more physical than ours. Another contributing factor may be the approximate expression for the carbon EOS used by TFW, which overestimate the Coulomb effects, and makes their models less physical than ours in this regard. This leads to more compressible cores—the EOS is "softer"—and makes the TFW models contract more rapidly, leading to larger temperature gradients—and deeper convection zones—in the outer layers. We plan to examine these issues in more detail with the appropriate models in the future.

TABLE 1

THEORETICAL VALUES OF THE BLUE EDGE OF THE DB INSTABILITY STRIP VERSUS HELIUM LAYER MASS AND CONVECTIVE EFFICIENCY

Sequence	$(T_{\rm eff})_{\rm blue}$ (K)	$(T_{\rm eff})_{\rm mix}$ (K)
c60400ML1 BS	20,050	No mixing
c60600ML1 BS	20,130	13,000
c60800ML1 BS	20,150	16,500
c61000ML1 BS	Stable	17,000
c60200ML2 BS	22,200	No mixing
c60400ML2 BS	22,920	No mixing
c60600ML2 BS	23,120	14,500
c60600ML2 NBS	24,810	14,500
o60600ML2 BS	22,920	14,500
tc60600ML2 BS	22,800	14,500
c60700ML2 BS	22,990	18,000
c60800ML2 BS	22,730	18,000
c60900ML2 BS	Stable	18,500
c61000ML2 BS	Stable	19,000
c60400ML3 BS	24,900	No mixing
c60600ML3 BS	24,810	15,000
c60600ML3 NBS	27,100	15,000
c60800ML3 BS	24,280	19,000
c61000ML3 BS	Stable	21,500

NOTES.—ML1 stands for the convection prescription of Böhm-Vitense 1958 with time mixing-length/presssure scale height ratio ($\equiv\alpha$) set to unity. ML2 stands for the convection prescription of Böhm & Cassinelli 1971 with the mixing-length/pressure scale height ratio ($\equiv\alpha$) set to unity. ML3 is the same as ML2, except $\alpha = 2$. BS means we use the convective efficiency prescription of Böhm & Stückl 1967. NBS indicates that we do not use it.

Our pulsationally unstable models show a trend of increasing growth rates with decreasing helium layer mass. However, when $M_{\rm He} \lesssim 10^{-8}M_*$ (see below), models with thicker helium layers have larger eigenfunction amplitudes just below the driving region. The larger amplitudes result in higher kinetic energies and smaller growth rates, because the growth rate is inversely proportional to the kinetic energy (Cox 1980; Winget 1981; Kawaler 1986; Unno et al. 1989). Trapped modes have the smallest kinetic energies, so they have the largest growth rates. The fact that trapped modes have the largest growth rates also supports the hypothesis of Winget, Van Horn, & Hansen (1981) that trapped modes should have larger amplitudes—based on linear pulsation theory. However, recent observations demonstrate that this hypothesis is probably not valid for GD 358.

When the mass of the helium layer in our models drops below $10^{-8}M_*$, they are all pulsationally stable between 30,000 and 19,000 K. The eigenfunctions of models where $M_{\rm He} < 10^{-8}M_*$ have larger amplitudes (compared to models with thicker helium layers) in the radiative damping region located just below the driving region (see Fig. 2, *top panel*). This *increased damping* stabilizes our models when $M_{\rm He} < 10^{-8}M_*$. The increased eigenfunction amplitude in the damping region[2] (see Fig. 2, *middle panel*) is caused by the presence of a convection zone at the He/C interface (see Fig. 2, *bottom panel*) of models with very thin helium layers. Coupled with the upper mass limit for the helium layer of $10^{-2}M_*$, this result limits the range of allowable helium layer masses to $10^{-2}M_* \gtrsim M_{\rm He} \gtrsim 10^{-8}M_*$. The inferred mass of the helium layer from the carbon pollution problem (Pelletier et al. 1986) at $10^{-3.5\pm0.5}M_*$ falls within our allowable mass range. If the helium layer mass in the DB white dwarf is thinner than $10^{-8}M_*$, the helium and carbon would eventually mix (Pelletier et al. 1986), leading to white dwarf atmospheres dominated by carbon. Observations to date do not reveal any signs of these objects. Either they do not exist, or their numbers are so small that only a very small fraction of the DB white dwarfs have $M_{\rm He} < 10^{-8}M_*$.

While the blue edge is not sensitive to the helium layer mass, it *is* sensitive to the total stellar mass, moving to hotter temperatures as we increase the mass of the models (see Table 2 and Fig. 3). At a given effective temperature, lower luminosities cause the thermal timescale in the driving region to increase with increasing stellar mass, resulting in hotter blue edges.

[2] While the eigenfunction amplitude is slightly larger, it is not *obvious* that this should be responsible for the large amount of damping seen when $M_{\rm He} = 10^{-10}M_*$. We feel our physical description is correct, but some other unappreciated factor may also play a role here.

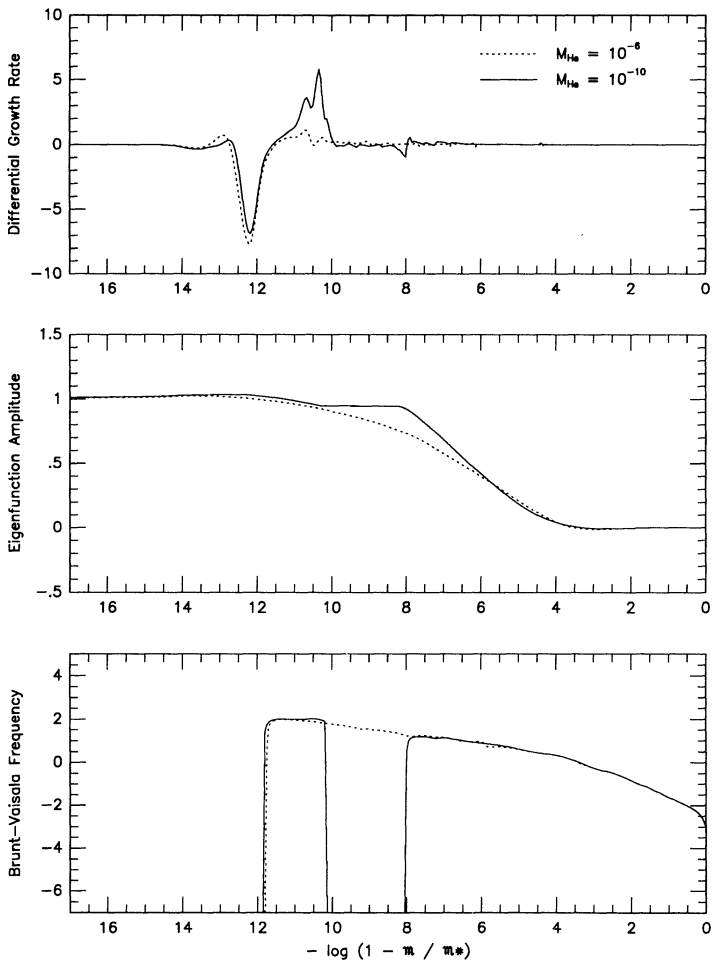

FIG. 2.—Tentative explanation for the minimum helium layer mass required for pulsational instability in our DB models. We plot $l = 2$, $k = 3$ eigenfunctions for models with $M_{He} = 10^{-6} M_*$ (*dashed line*) and $M_H = 10^{-10} M_*$ (*solid line*) near 24,000 K. The differential contribution to the growth rate (*top panel*) shows a region of strong damping just below the driving region in the c61000ML3 model. The y_2 (horizontal perturbation) eigenfunction (*middle panel*) for the c61000ML3 model has a slightly larger amplitude in these areas, which lies within the region of radiative damping (hatched area in bottom panel) just below the driving region. The extra damping prevents pulsational instabilities from occurring.

Also, the pulsation periods drop with increasing mass, enhancing movement of the blue edge to higher effective temperatures. As a result, our 0.8 $M_\odot$ blue edge is about 1200 K to 2500 K hotter than the 0.6 $M_\odot$ blue edge, similar to the expectations of Winget et al. (1983). Our 0.4 $M_\odot$ ML2 sequence has a blue edge of ~20,000 K, below the observed red edge. The very low blue edge temperature is the combined result of the pulsation periods being longer in a lower mass model and the smaller thermal timescale at a given mass point and effective temperature in a lower mass model. Based on our results and the observational constraints on the helium layer mass, we suggest

TABLE 2

THEORETICAL VALUES OF THE BLUE EDGE OF THE DB INSTABILITY STRIP VERSUS STELLAR MASS

Sequence	$(T_{eff})_{blue}$ (K)	$(T_{eff})_{mix}$ (K)
c40600ML2 BS	20,620	15,000
c50600ML2 BS	21,950	15,000
c60600ML2 BS	23,120	14,500
c70600ML2 BS	23,610	No mixing
c80600ML2 BS	25,690	No mixing
c60600ML3 NBS	27,100	15,000
c70600ML3 NBS	27,800	13,000
c80600ML3 NBS	28,300	No mixing

NOTE.—See notes after Table 1 for explanation of symbols.

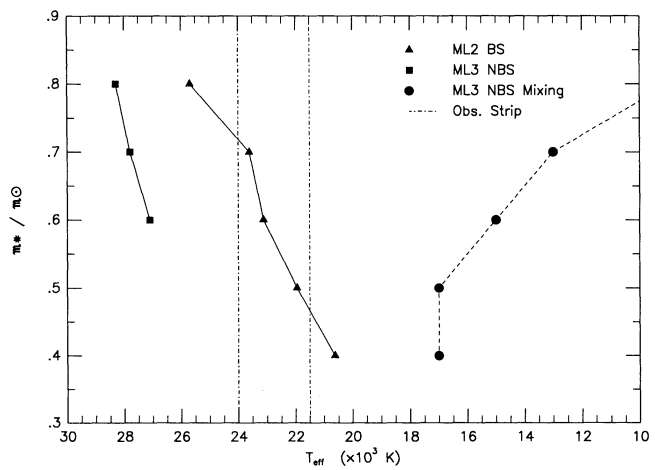

FIG. 3.—Location of the blue edge of the theoretical DB instability strip as a function of stellar mass. The theoretical blue edge for our 0.4 $M_\odot$ models lies below the red edge of the observed instability strip, suggesting that these stars will not pulsate.

that any *nonvariable* DB stars found within the instability strip either have an unfavorable pulsation axis inclination angle or low masses.

The hottest known DBV star is GD 358, with a temperature of $24 \pm 1 \times 10^3$ K (Thejl et al. 1991; Koester et al. 1985). GD 358 has a complicated pulsation spectrum (Winget et al. 1994) with long-period (≥ 700 s) modes excited; both suggest the actual observational DB blue edge is somewhat hotter than GD 358. Given this, we consider 25,000 K to be a reasonable guess for the observed blue edge, which we can match using models with efficient (ML2 NBS or ML3 BS) convection. High-quality UV spectra of the DBV stars from *Hubble Space Telescope* should refine the observed blue edge temperature. This, along with improved convection theories should settle the question of how to model the convection zone of DB white dwarfs.

The observations of Thejl et al. also suggest a red edge near 21,500 K. Our 0.6 $M_\odot$ models have a red edge near 18,500 K when we use ML3 NBS convection and the red edge drops to ~17,000 K with ML2 NBS convection. Our theoretical instability strips are about 6000 K, wider than the 3000–4000 K width of the observed instability strip. We speculate this difference may be because we do not include perturbations of the convective flux in our pulsation analysis programs.

3.2. *DAV Model Results*

We start by examining the location of the blue edge as we vary the hydrogen layer mass, the helium layer mass, and the convective efficiency. Then we examine the dependence of the blue edge on stellar mass and compare our blue edges with the observational data and other theoretical calculations. Finally, we discuss the red edge of the instability strip.

We find *no significant change in the blue edge of our DA models when we vary the hydrogen layer mass* from $10^{-4}M_*$ to $10^{-12}M_*$ (see Table 3 and Fig. 4). If we look at the growth rates for models with differing hydrogen layer masses, there is a trend toward larger growth rates with decreasing hydrogen layer mass (see Fig. 5), although mode trapping effects are strong. Our model with $M_H = 10^{-4}M_*$ clearly show smaller growth rates than models with thinner hydrogen layers, and there are fewer unstable modes. However, the growth rates for

TABLE 3

THEORETICAL VALUES OF THE BLUE EDGE OF THE DA INSTABILITY STRIP VERSUS HYDROGEN LAYER MASS, HELIUM, LAYER MASS, AND CONVECTIVE EFFICIENCY

Sequence	$(T_{\rm eff})_{\rm blue}$ (K)
Hydrogen Layer Mass	
c60204ML3 NBS	12,460
c60406ML3 NBS	12,550
c60408ML3 NBS	12,520
c60410ML3 NBS	12,770
c60412ML3 NBS	12,550
Helium Layer Mass	
c60210ML3 NBS	12,630
c60410ML3 NBS	12,770
c60610ML3 NBS	12,640
c60810ML3 NBS	12,470
Convective Efficiency	
c60410ML1 BS	10,090
c60410ML1 NBS	10,790
c60410ML1 ($\alpha = 2.5$) NBS	12,100
c60410ML1 ($\alpha = 3$) NBS	12,440
c60410ML2 NBS	11,670
c60410ML3 BS	11,710
c60410ML3 NBS (Pure H opacs)	12,720

NOTE.—See notes after Table 1 for explanation of symbols.

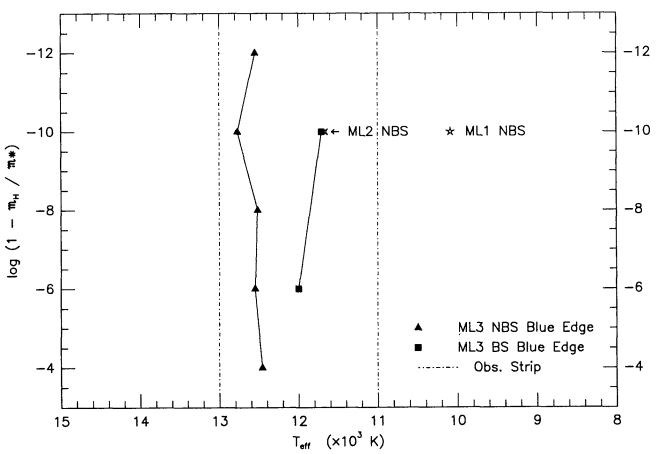

FIG. 4.—Location of the blue edge of the theoretical DA instability strip as a function of hydrogen layer mass and convective efficiency. Models with ML3 (very efficient) convection best match the observed blue edge (*dashed-dotted line*). The theoretical blue edge does not depend on the hydrogen layer mass.

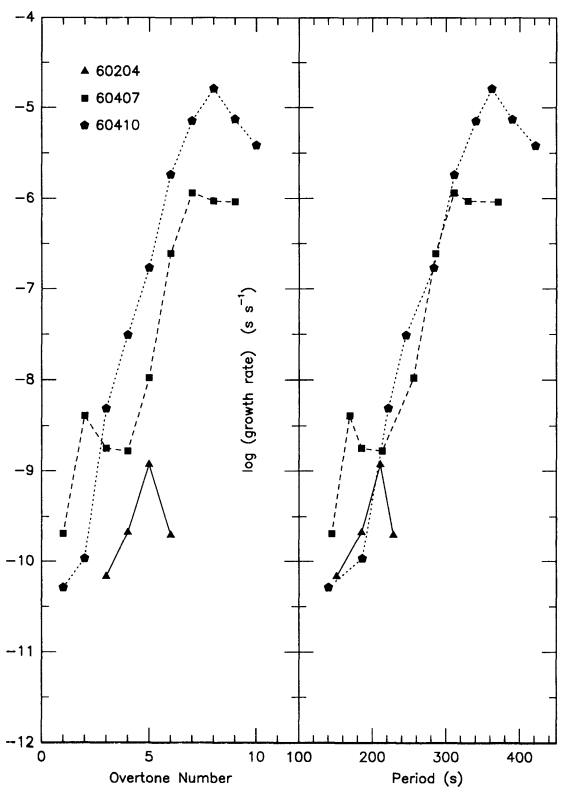

FIG. 5.—Growth rate trends for $l = 2$ modes in DA models with differing hydrogen layer masses. In this figure, the models are near 12,300 K and have hydrogen layer masses of $10^{-4}M_*$, $10^{-7}M_*$, and $10^{-10}M_*$. Local maxima in the growth rates of the two models with the thinnest hydrogen layer masses are due to mode trapping. Ignoring this effect, there is a trend toward larger growth rates with decreasing hydrogen layer mass.

models with $M_H = 10^{-7}M_*$ can be larger than those of a model with $M_H = 10^{-8}M_*$ due to mode trapping effects. Except for the first few modes—where mode trapping dominates in thicker hydrogen layers—the growth rates are largest when $M_H = 10^{-10}M_*$ (see Fig. 5). When $M_H = 10^{-12}M_*$, the growth rates become smaller because of the influence of the convection zone at the H/He interface, in analogy to the more extreme case exhibited by the DB models when $M_{He} \lesssim 10^{-8}M_*$.

This trend shows the hydrogen layer mass affects the magnitude of the growth rate, and this is due to the increased amplitude of the eigenfunctions in the strong radiative damping region as we increase the hydrogen layer mass (Winget & Fontaine 1982). This effect is physical, and we see it in our models and those of TFW, which we reanalyzed. Whether or not this trend also shows up as a *change in the sign* of the growth rate is not clear. Previous studies (Winget et al. 1982; Cox et al. 1987; and Bradley et al. 1989) gave conflicting results. Our reanalysis of the TFW models used by Winget et al. (1982) and Bradley et al. (1989) show that the sign of the growth rate in models near the blue edge is quite sensitive to the zoning, casting doubt on the reliability of their results. However, our growth rates using the new models created by WDEC do not suffer sign changes as we vary the zoning. The magnitude of the growth rate can change by a factor of 2, but this is consistent with difference between the eigenvalue and variational principle growth rate values. A definitive answer to the effect of the hydrogen layer mass on the sign of the growth rate must await nonadiabatic calculations that correctly include convection-pulsation interactions. Until then, our results suggest that the hydrogen layer mass does not affect the sign of the growth rate.

There is no change in the blue edge when we vary helium layer mass between $10^{-2}M_*$ and $10^{-8}M_*$ (see Table 3). Even with a helium layer as thin as $10^{-8}M_*$, there is negligible driving at the He/C interface (see Fig. 6, *top panel*). The thermal timescale (Fig. 6, *dashed line*, *bottom panel*) at the He/C interface is $\sim 10^8$ s, far longer than the 233 s pulsation period of the $l = 2$, $k = 3$ mode of our example. The driving and damping region near $10^{-10}M_*$ is associated with the H/He interface; the driving and damping from this region average out to make a neutral contribution to the overall pulsational instability of the mode. The physical behavior of both of these features results from their lying well below the adiabatic/nonadiabatic transition located near $10^{-12}M_*$ in this model. The eigenfunction shapes and the pulsation periods can be affected by the helium layer mass because the main region of period formation lies between $10^{-4}M_*$ and $10^{-10}M_*$, which is below the adiabatic nonadiabatic transition region.

In contrast to the hydrogen and helium layer mass, the convective efficiency has a strong effect on the location of the blue edge. Inefficient convection (such as ML1) yields blue edges below 11,000 K, while our most efficient version of convection (ML3 NBS) produces blue edges around 12,550 K. Use of the Böhm-Stückl prescription drops the blue edge temperature from 700 to 1000 K for all the mixing-length versions we consider (see Table 3).

The theoretical blue edge also depends on the stellar mass, ranging from 12,000 K for our 0.4 $M_\odot$ models up to 13,500 K for our 0.8 $M_\odot$ models (see Table 4 and Fig. 7) for our most efficient version of convection. These results confirm and extend the trend found by Winget (1981). We also find no appreciable variation in the blue edge temperature when we vary the hydrogen layer mass in our 0.5 and 0.7 $M_\odot$ models

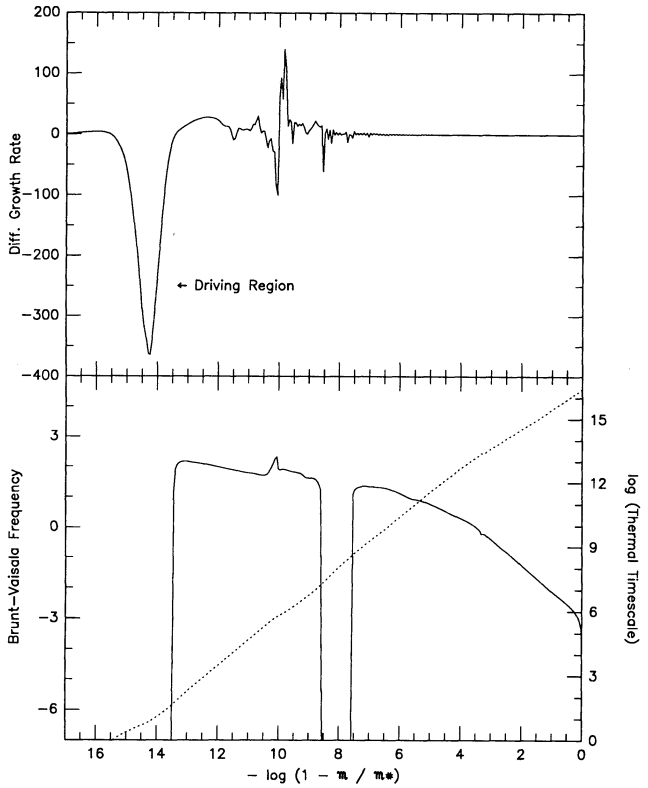

FIG. 6.—Pulsation driving properties of an $l = 2$, $k = 3$ mode from a c60810ML3 NBS model at 12,380 K. Even with a helium layer this thin, there is a negligible amount of driving (*top panel*) at $10^{-8}M_*$, where the He/C interface lies. The thermal timescale (*dashed line*, *bottom panel*) at the He/C interface is $\sim 10^8$ s, far longer than the pulsation period of 233 s for this mode.

(see Table 4), confirming the trend found in our 0.6 $M_\odot$ models.

The observations (see Wesemael et al. 1991, and references therein) all point to a blue edge near 13,000 K, implying a convective efficiency greater than ML3 without the Böhm-Stückl prescription in 0.6 $M_\odot$ models. More recent results (Kepler & Nelan 1993) suggest a significantly cooler blue edge near 12,300 K; our 0.6 $M_\odot$ models with very efficient convec-

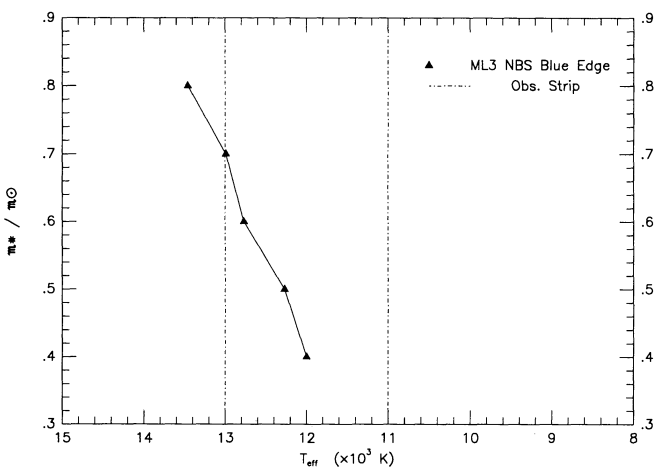

FIG. 7.—Location of the blue edge of the theoretical DA instability strip as a function of stellar mass. The theoretical blue edge for all masses we consider lie within the observed instability strip.

TABLE 4

THEORETICAL VALUES OF THE BLUE EDGE OF THE DA INSTABILITY STRIP VERSUS STELLAR MASS

Sequence	$(T_{\rm eff})_{\rm blue}$ (K)
c40410ML3 NBS	12,000
c50406ML3 NBS	12,220
c50408ML3 NBS	12,310
c50410ML3 NBS	12,270
c60410ML3 NBS	12,770
c70406ML3 NBS	12,890
c70408ML3 NBS	12,920
c70410ML3 NBS	12,990
c80410ML3 NBS	13,460

NOTE.—See notes to Table 1 for explanation of symbols.

tion can duplicate this. Our hottest 0.6 $M_\odot$ blue edge is about 300–500 K cooler than the 13,000 K found by Bradley et al. (1989). Finally, Kawaler (1993) finds a blue edge of 12,700 K of 0.6 $M_\odot$ static models with $M_{\rm H} = 10^{-10} M_*$, almost identical to our value. Thus, despite the different physics involved, the theoretical blue edges agree to within 300–500 K when we use the same description of convection.

The 300–500 K difference between our results and those of Bradley et al. (1989) may be significant, because it represents about 20% of the observed width of the DAV instability strip. Assuming the difference to be significant, we have two alternative explanations for it. Like the DB models, the difference is either due to the usage of an approximate EOS in the cores of the TFW models or our neglect of gravitational contraction effects in the static envelopes of our models.

Our blue edges are hotter than those of Cox et al. (1987), but we use more efficient prescriptions for convection. For a more straightforward comparison to the models of Cox et al., we construct 60410 sequences using non Böhm-Stückl ML1 convection with $\alpha = 1.0$, 2.5, and 3.0. Our resultant blue edges are 10,790 K ($\alpha = 1$), 12,100 K ($\alpha = 2.5$), and 12,440 K ($\alpha = 3$). Our $\alpha = 1$ blue edge is consistent with theirs, the blue edges for our $\alpha = 2.5$ and 3 sequences are hotter than their values of 11,500 to 12,000 K for $\alpha = 3$. A comparison of convection zone properties show that ours are considerably deeper; most of this difference is likely due to differences in the hydrogen EOS tables, since we find virtually no difference in the blue edge temperature (12,720 vs. 12,770 K) when we use the pure hydrogen opacity table in Cox & Tabor (1976), compared to our standard hydrogen table where $Z = 0.001$.

We are unable to find a red edge with our DA models, although the models drop back toward neutral stability after about a 1000 K span of instability. We do not consider convection/pulsation interactions or convective mixing of the hydrogen layer into the underlying helium layer, both of which have been suggested as the mechanism responsible for stability at the red edge.

4. SUMMARY

The theoretical blue edges of our DB and DA models are *insensitive to the surface layer masses.* We also find the blue edge is insensitive to the thickness of the H/He or He/C transition zone, and to the core composition. The only exception is the discovery of a minimum helium layer mass required for pulsational instability in our DB models, located at $M_{\rm He} = 10^{-8} M_*$.

There is a trend toward larger growth rates with decreasing helium layer mass in our DB models, and with decreasing hydrogen layer mass in our DA models. The growth rate trend in our DA models is strongly affected by mode trapping, however. Mode trapping also causes trapped modes to have the largest growth rates, and by extension of linear theory, they should also have the largest observed amplitudes. The observations of GD358 (a DBV star) do not support this hypothesis, although we cannot rule out the possibility that it holds for ZZ Ceti white dwarfs.

The blue edge is very sensitive to the assumed convective efficiency. We need a description of convection at least as efficient as the ML2 version without the Böhm-Stückl prescription of ML3 with Böhm-Stückl to match the observed DB blue edge. Matching the observed DA blue edge requires even more efficient convection; ML3 without Böhm-Stückl comes closest for our 0.6 $M_\odot$ models.

The theoretical blue edge for both DA and DB models moves to hotter temperatures as we increase the stellar mass, depending on the convective efficiency used. Our 0.5 to 0.8 $M_\odot$ DB models with efficient convection have blue edges between 24,000 and 28,000 K, consistent with the observations, while our 0.4 $M_\odot$ DBV models with ML2 convection have blue edges near 20,000 K, below the observed red edge. Based on these results, we suggest that any nonvariable DB white dwarfs found have unfavorable viewing geometries or low masses. Our DA models with very efficient convection and masses ranging from 0.4 to 0.8 $M_\odot$ have blue edges ranging from 12,000 to 13,500 K. The blue edges of our 0.6 to 0.8 $M_\odot$ models are the most similar to observational values, and possible presence of nonvariables within the instability strip may be due to low mass DA white dwarfs that have not reached the blue edge for their mass yet.

We are grateful to C. J. Hansen, S. D. Kawaler, R. E. Nather, and M. A. Wood for their encouragement and many discussions. We also wish to thank S. D. Kawaler for sending us blue edge results in advance of publication. P. A. B. wishes to thank the University of Texas for a graduate student fellowship during the past 2 years that allowed him to work with a minimum of distractions. This research was supported by the National Science Foundation under grants 86-00507 and 90-14655 through the University of Texas and McDonald Observatory.

REFERENCES

Arcouragi, J.-P., & Fontaine, G. 1980, ApJ, 242, 1208
Bergeron, P., Saffer, R. A., & Liebert, J. 1992a, ApJ, 394, 228
Bergeron, P., Wesemael, F., & Fontaine, G. 1992b, ApJ, 387, 288
Bergeron, P., Wesemael, F., Fontaine, G., & Liebert, J. 1990, ApJ, 351, L21
Blöcker, T., & Schönberner, D. 1991, in Proc. 7th European Workshop on White Dwarfs, ed. G. Vauclair & E. M. Sion (NATO ASI Ser.) (Dordrecht: Kluwer), 1
Böhm, K.-H., & Cassinelli, J. 1971, A&A, 12, 21
Böhm, K.-H., & Stückl, E. 1967, Z. Astrophys., 66, 487
Böhm-Vitense, E. 1958, Z. Astrophys., 46, 108
Bradley, P. A., & Winget, D. E. 1991, ApJS, 75, 463
Bradley, P. A., Winget, D. E., & Wood, M. A. 1989, in IAU Colloq. 114, White Dwarfs, ed. G. Wegner (Berlin: Springer), 286
———. 1992, ApJ, 391, L33
———. 1993, ApJ, 406, 661 (BWW)
Brassard, P., Fontaine, G., Wesemael, F., Kawaler, S. D., & Tassoul, M. 1991, ApJ, 367, 601
Brassard, P., Fontaine, G., Wesemael, F., & Tassoul, M. 1992, ApJS, 81, 747
Brickhill, A. J. 1983, MNRAS, 204, 537
———. 1991, MNRAS, 251, 673
Canuto, V. M., & Mazzitelli, I. 1991, ApJ, 370, 295
Carroll, B. W. 1981, Ph.D. thesis, Univ. Colorado

Cox, A. N., & Hollowell, D. E 1991, in Proc. 7th European Workshop on White Dwarfs, ed. G. Vauclair & E. M. Sion (NATO ASI Ser.) (Dordrecht: Kluwer), 211
Cox, A. N., Starrfield, S. G., Kidman, R. B., & Pesnell, W. D. 1987, ApJ, 317, 303
Cox, A. N., & Tabor, J. E. 1976, ApJS, 31, 271
Cox, J. P. 1980, Theory of Stellar Pulsation (Princeton Univ. Press)
D'Antona, F., & Mazzitelli, I. 1990, ARA&A, 28, 139
———. 1991, in IAU Symp. 145, Evolution of Stars: the Photospheric Abundance Connection, ed. G. Michaud & A. Tutukov (Dordrecht: Kluwer), 399
Daou, D., Wesemael, F., Bergeron, P., Fontaine, G., & Holberg, J. B. 1990, 364, 242
Dolez, N., Vauclair, G., & Koester, D. 1991, in Proc. 7th European Workshop on White Dwarfs, ed. G. Vauclair & E. M. Sion (NATO ASI Ser.) (Dordrecht: Kluwer), 361
Dziembowski, W. 1977, Acta Astron., 27, 203
Epstein, I. 1950, ApJ, 112, 6
Fontaine, G., & Wesemael, F. 1987, in IAU Colloq. 95, The Second Conference on Faint Blue Stars, ed. A. G. D. Philip, D. S. Hayes, &. J. Liebert (Schenectady: Davis), 319
———. 1991, in IAU Symp. 145, Evolution of Stars: the Photospheric Abundance Connection, ed. G. Michaud & A. Tutukov (Dordrecht: Kluwer), 421
Fontaine, G., Bergeron, P., Lacombe, R., Lamontagne, R., & Talon, A. 1985, AJ, 90, 1094
Greenstein, J. L. 1986, ApJ, 304, 334
Hansen, C. J., Winget, D. E., & Kawaler, S. D. 1985, ApJ, 297, 544
Iben, I., Jr. 1991, ApJS, 76, 55
Kawaler, S. D. 1986, Ph.D. thesis, Univ. Texas
———. 1990, in Confrontation Between Stellar Pulsation and Evolution, ed. C. Cacciari & G. Clementini (Provo: ASP), 494
———. 1993, ApJ, 404, 294
Kawaler, S. D., & Hansen, C. J. 1989, in IAU Colloq. 114, White Dwarfs, ed. G. Wegner (Berlin: Springer), 97
Kawaler, S. D., Hansen, C. J., & Winget, D. E. 1985, ApJ, 295, 547
Kepler, S. O., & Nelan, E. P. 1993, AJ, 105, 608
Koester, D., & Schönberner, D. 1986, A&A, 154, 125
Koester, D., Vauclair, G., Dolez, N., Oke, J. B., Greenstein, J. L., & Weidemann, V. 1985, A&A, 149, 423
Lamb, D. Q., & Van Horn, H. M. 1975, ApJ, 200, 306
Lamontagne, R., Wesemael, F., Fontaine, G., Wegner, G., & Nelan E. P. 1989, in IAU Colloq. 114, White Dwarfs, ed. G. Wegner (Berlin: Springer), 240
Liebert, J., Wesemael, F., Hansen , C. J., Fontaine, G., Shipman, H. L., Sion, E. M., Winget, D. E., & Green, R. F. 1986, ApJ, 309, 241
Mazzitelli, I., & D'Antona, F. 1991, in Proc. 7th European Workshop on White Dwarfs, ed. G. Vauclair & E. M. Sion (NATO ASI Ser.) (Dordrecht:Kluwer), 305
Oke, J. B., Weidemann, V., & Koester, D. 1984, ApJ, 281, 276
Osaki, Y., & Hansen, C. J. 1973, ApJ, 185, 277
Pelletier, G., Fontaine, G., Wesemael, F., Michaud, G., & Wegner, G. 1986, ApJ, 307, 242
Pesnell, W. D. 1990, ApJ, 363, 227
Philip, A. G. D., Hayes, D. S., & Liebert, J., eds. 1987, IAU Colloq. 95, The Second Conference on Faint Blue Stars (Schenectady: Davis)
Saio, H., & Cox, J. P. 1980, ApJ, 236, 549
Stanghellini, L., Cox, A. N., & Starrfield, S. G. 1991, ApJ, 383, 766
Tassoul, M., Fontaine, G., & Winget, D. E. 1990, ApJS, 72, 335 (TFW)
Thejl, P., Vennes, S., & Shipman, H. L. 1991, ApJ, 370, 355
Unno, W., Osaki, Y., Ando, H., Saio, H., & Shibahashi, H. 1989, Nonradial Oscillations of Stars, 2d ed. (Tokyo: Univ. Tokyo Press)
Vauclair, G., & Sion, E. M., eds. 1991, Proc. 7th European Workshop on White Dwarfs (NATO ASI Ser.) (Dordrecht: Kluwer)
Vennes, S., & Fontaine, G. 1992, ApJ, 401, 288
Wegner, G., ed. 1989, IAU Colloq. 114, White Dwarfs (Berlin: Springer)
Wesemael, F., Bergeron, P., Fontaine, G., & Lamontagne, R. 1991, in Proc. Seventh European Workshop on White Dwarfs, ed. G. Vauclair & E. M. Sion (NATO ASI Ser.) (Dordrecht: Kluwer), 159
Wesemael, F., Lamontagne, R., & Fontaine, G. 1986, AJ, 91, 1376
Winget, D. E. 1981, Ph.D. thesis, Univ. Rochester
———. 1988a, in IAU Symp. 123, Advances in Helio- and Asteroseismology, ed. J. Christensen-Dalsgaard & S. Frandsen (Dordrecht: Reidel), 305
———. 1988b, in Proc. Multimode Stellar Pulsations, ed. G. Kovács, L. Szabados, & B. Szeidl (Budapest: Konkoly Obs.), 181
———. 1991, in Proc. 7th European Workshop on White Dwarfs, ed. G. Vauclair & E. M. Sion (NATO ASI Ser.) (Dordrecht: Kluwer), 129
———. 1993, in Proc. 8th European Workshop on White Dwarfs, ed. M. A. Barstow (NATO ASI Ser.) (Dordrecht: Kluwer), 449
Winget, D. E., & Fontaine, G. 1982, in Pulsations in Classical and Cataclysmic Variable Stars, ed. J. P. Cox & C. J. Hansen (Boulder: Univ. Colorado), 46
Winget, D. E., Van Horn, H. M., & Hansen, C. J. 1981, ApJ, 245, L33
Winget, D. E., Van Horn, H. M., Tassoul, M., & Fontaine, G. 1983, ApJ, 268, L33
Winget, D. E., Van Horn, H. M., Tassoul, M., Hansen, C. J., Fontaine, G., & Carroll, B. W. 1982, ApJ, 252, L65
Winget, D. E., et al. 1994, in preparation
Wood, M. A. 1990, Ph.D. thesis, Univ. Texas
———. 1992, ApJ, 386, 539